IEEE Access
Multidisciplinary | Rapid Review | Open Access Journal

Received March 18, 2020, accepted April 13, 2020, date of publication April 20, 2020, date of current version May 6, 2020.

Digital Object Identifier 10.1109/ACCESS.2020.2988656

Passivity-Based Control With Active Disturbance Rejection Control of Vienna Rectifier Under Unbalanced Grid Conditions

JIANGUO LI[1], (Member, IEEE), MIAN WANG[2], (Student Member, IEEE), JING WANG[3], YAJING ZHANG[1], DAOKUAN YANG[1], JIUHE WANG[1], AND YUMING ZHAO[3]

[1]School of Automation, Beijing Information Science and Technology University, Beijing 100192, China
[2]School of Electrical Engineering, Beijing Jiaotong University, Beijing 100044, China
[3]Shenzhen Power Supply Corporation, Shenzhen 518048, China

Corresponding author: Jianguo Li (lijianguo@bistu.edu.cn)

This work was supported in part by the Beijing Natural Science Foundation under Grant 3202010/3204040, in part by the National Natural Science Foundation under Grant 51777012, in part by the Natural Science Foundation of Beijing—Education Committee Joint Funding Project under Grant KZ201911232045, and in part by the Key Science and Technology Projects of China Southern Power Grid Corporation under Grant 090000KK52180116.

ABSTRACT In this paper, a practical passivity-based control (PBC) with active disturbance rejection control (ADRC) is proposed to improve performance of the Vienna rectifier under unbalanced grid conditions. In general, the traditional double-loop control based on positive and negative sequence transformation is used in Vienna rectifier under unbalanced grid conditions. However, it could not fundamentally solve the additional time delay caused by the second harmonic filter and loss of performance caused by a linear weighted sum of proportional integral (PI) controller. What's more, the complexity of the controller is high for the positive and negative sequence currents need to be controlled separately. The PBC is a nonlinear controller based on energy dissipation and it has strong robustness to interference. Further, the line voltage based PBC in inner current loop can deal with the voltage unbalance effectively and easily without negative sequence transformation. To improve the disturbance rejection ability, the ADRC is applied in outer voltage loop, which could overcome PI's drawbacks of step overshoot and slow response. Under unbalanced grid conditions, the proposed control strategy has good performance, easy implementation and less consuming time with PBC control in inner current loop, and it has strong robustness and fast track performance with ADRC control in outer voltage loop. The detailed mathematical model, control principle and controller design of the Vienna rectifier are thoroughly analyzed. In addition, simulation results based on SIMULINK are also given in the paper. Finally, a downsize 5kW Vienna rectifier prototype is built to validate the correctness and effectiveness of the proposed strategy.

INDEX TERMS Active disturbance rejection control, passivity-based control, unbalanced grid condition, Vienna rectifier.

I. INTRODUCTION

The Vienna rectifier, which was proposed by Johann W. Kolar in 1997, needs only one power switch in one phase, which has no dead time effect and shares only half of the dc voltage stress. What's more, it can realize perfect sinusoidal current and unity power factor with high reliability and high power-density. Thus, it is widely applied in the unidirectional rectifier, such as active power filter, power factor correction, communication power supply, uninterrupted power supply, electric vehicle charging and new energy power generation [1], [2].

A voltage unbalance often happens in the power system because of unbalanced load or nonlinear load. Here voltage unbalance means unequal voltage magnitudes at the fundamental frequency (under-voltages or over-voltages), harmonic distortion and dc offset injection. In other words, the three-phase voltages are not sinusoidal or unequal in magnitude. According to [3], the voltages unbalance factor of many grids exceeds 3% in the U.S. But the grid voltage

The associate editor coordinating the review of this manuscript and approving it for publication was Ahmad Elkhateb.

unbalance factor must be less than 2% during a long period of time according to the IEC standard. Excessive voltage unbalance can lead to Vienna rectifier disturbance such as over current, over temperature, output voltage fluctuation and so on. It may even cause the Vienna rectifier to fail to work normally [4]–[6].

In general, the Vienna rectifier is controlled as a positive sequence voltage source [7]–[9], and it works normally under balanced grid conditions. Unfortunately, the control technique of the Vienna rectifier faces the challenge for the negative sequence current, which will be generated under unbalanced grid conditions and threats the safe operation of the Vienna rectifier. Usually, positive and negative sequence transformations are used in traditional current controllers to detect positive and negative sequence currents. And then two currents controllers are used to regulate the positive and negative currents respectively [10], [11]. Although the sequence currents controllers are effective under unbalanced grid conditions, the controllers suffer from additional time delay caused by second harmonic filter, they are more complex because of the need to calculate and control multi parameters, and they are also easily affected by high order harmonics [12]–[14].

Normally, a double-loop based control strategy is used in Vienna rectifier system, which consists of an outer voltage loop and an inner current loop. For inner current loop, a proportional integral (PI) control is initially used, but it is difficult to realize desired performance for the nonlinear Vienna rectifier [15]. The proportion resonant (PR) control can provide fast dynamic response with high stability, but it is too complex to implement in application [16], [17]. The hysteresis control (HC) and direct power (DP) control have simple control structures and fast dynamic responses, but their switching frequencies are not constant, and it is difficult to design their filters [18], [19]. The predictive control (PC) can eliminate forecast error and minimize resonant behavior, but it has the disadvantage of high sensitivity to parameters and heavy computation burden in application [20]. The dead beat (DB) control is one of predictive controls, and it has fast voltage and current regulation capability, but it also puts forward high requirements for the controller performance [21].

For outer voltage loop, a PI controller is normally used, but it has some weakness such as performance loss in the form of a linear sum and complications brought by the integral control. In this paper, an active disturbance rejection control (ADRC) controller is used in the outer voltage loop to guarantee fast tracking and robustness of the system, line voltages based passivity-based control (PBC) controller is used in the inner current loop to guarantee stability and dynamic performance of the system under unbalanced conditions, and the PBC with ADRC control strategy is thoroughly discussed.

The PBC strategy, which was proposed by R. Ortega and M. Spong in 1989 [22], is a nonlinear control based on energy dissipation, it utilizes energy dissipation to control stability and track given object by means of damping injection. PBC has strong robustness to system parameters deviation and external interference, and it is easily designed and controlled in application. In the electrical application, PBC is used in power conversion system, rectifier, photovoltaic inverter, motor drive, static synchronous compensator, dynamic voltage restorer and dc-dc converter [23]–[27]. Compared with linear control and other nonlinear control strategies, line voltages based PBC control strategy in inner current loop can be easily designed and realized, and be expected to improve Vienna rectifier's static and dynamic performance under unbalanced grid conditions.

The ADRC strategy, which was proposed by J. Han in 1980s [28], is a nonlinear robust control strategy, it is driven by estimation error and tracking error, and it can actively estimate and compensate internal dynamic changes and external disturbances in real time. In the electrical application, ADRC is used in dc-dc converter, gyroscopes, permanent magnet synchronous motor and flywheel energy storage system [29]–[32]. Compared with PI control strategy, ADRC control strategy in outer voltage loop is expected to provide the desired current for the inner current loop and improve Vienna rectifier's strong robustness and fast track performance.

In the study, a practical PBC with ADRC control strategy is proposed to improve performance of the Vienna rectifier under unbalanced grid conditions. The Vienna rectifier topology is analysed thoroughly, and the line voltage based mathematical model in Euler Lagrange (EL) form is deduced. In addition, the passivity characteristic of Vienna rectifier is demonstrated, and the implementation differential equations are given. Further, a PBC with ADRC based controller is designed. Besides, the simulation verification based on SIMULINK is carried out, and the downsized 5 kW prototype experiments further verify the proposed control strategy for Vienna rectifier. The rest of this study is organized as follows. In Section II, the Vienna rectifier topology is introduced and analysed thoroughly. In Section III, the mathematical model based on EL equation is proposed. In Section IV, the PBC with ADRC based controller is designed according to the EL model. Later in Section V and VI, the results of simulation and prototype experiment are given separately. Finally, Section VII concludes the study.

II. VIENNA RECTIFIER TOPOLOGY ANALYSIS

A. VIENNA RECTIFIER TOPOLOGY

The Vienna rectifier is made up of L, R, SW_i, VD_{i1}, and VD_{i2} ($i = a$, b, and c), as depicted in the Fig. 1. Where L and R are lumped inductor and equivalent resistor, respectively. SW_i is phase i bidirectional power switch. VD_{i1} and VD_{i2} are phase i power diodes.

B. VIENNA RECTIFIER PRINCIPLE

It is assumed that all the components are ideal. Taking the phase i for example, when the power switch

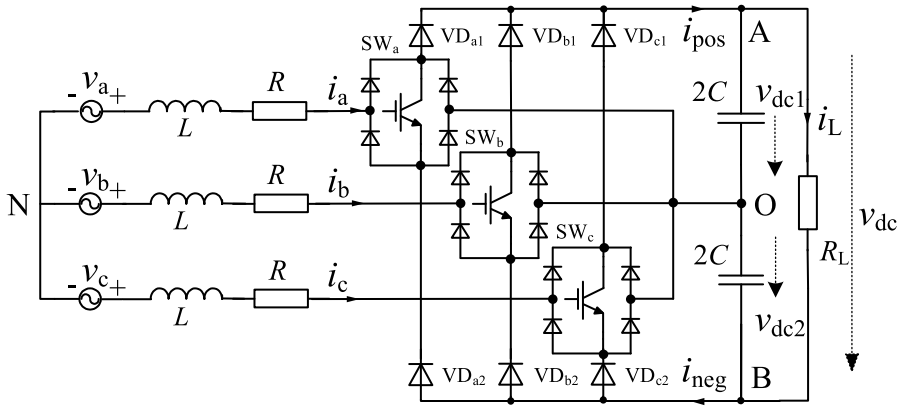

FIGURE 1. The Vienna rectifier topology.

SW_i is on, the phase i is clamped to the dc midpoint (point O), and the Vienna ac voltage is equal to 0. When the power switch SW_i is off and the phase current is in positive direction, the power diode VD_{i1} will be on and the Vienna ac voltage is equal to v_{dc1}.When the power switch SW_i is off and the phase current is in negative direction, the power diode VD_{i2} will be on and the Vienna ac voltage is equal to -v_{dc2}. If defining the switching function as S_i, S_i can descript the Vienna rectifier states exclusively.

$$S_i = \begin{cases} +1 \; SW_i = 0, & i_i > 0 \\ 0 \; SW_i = 1 & i = a, b, c \\ -1 \; SW_i = 0, & i_i < 0 \end{cases} \tag{1}$$

According to modulation principle and KCL, the Vienna rectifier ac and dc voltages can be expressed as,

$$\begin{cases} v_{rio} = \dfrac{S_i v_{dc}}{2}[1 + sgn(i_i)\dfrac{\Delta v_{dc}}{v_{dc}}] \\ C\dfrac{dv_{dc}}{dt} = \dfrac{1}{2}\sum\limits_{i=a,b,c}^{S_i} i_i - \dfrac{v_{dc}}{R_L} \\ C\dfrac{d\Delta v_{dc}}{dt} = \dfrac{1}{2}\sum\limits_{i=a,b,c}^{S_i} \mathrm{sgn}(i_i) i_i \end{cases} \tag{2}$$

where v_{rio} is the Vienna rectifier ac voltage, v_{dc} and v_{dc} are the sum and difference voltages between the upper and lower capacitors, respectively, i.e. $v_{dc} = v_{dc1} + v_{dc2}$ and $v_{dc} = v_{dc1}$-v_{dc2}. sgn(x) is a sign function. when $x \geq 0$, sgn(x) is equal to 1, and when $x < 0$, sgn(x) is equal to -1. It is assumed that the dc capacitor voltages are absolutely balanced due to voltage balance control, then we can get,

$$\begin{cases} v_{rio} = \dfrac{S_i v_{dc}}{2} i = a, b, c \\ C\dfrac{dv_{dc}}{dt} = \dfrac{1}{2}(S_a i_a + S_b i_b + S_c i_c) - \dfrac{v_{dc}}{R_L} \end{cases} \tag{3}$$

III. VIENNA RECTIFIER MATHEMATICAL MODEL

A. ABC COORDINATE MODEL

According to KVL, the Vienna rectifier ac voltages and currents can be expressed as,

$$\begin{cases} L\dfrac{di_a}{dt} + Ri_a + v_{rao} + v_{ON} = v_a \\ L\dfrac{di_b}{dt} + Ri_b + v_{rbo} + v_{ON} = v_b \\ L\dfrac{di_c}{dt} + Ri_c + v_{rco} + v_{ON} = v_c \end{cases} \tag{4}$$

where v_{ON} is the potential difference between dc midpoint (point O) and the ac midpoint (point N).

Considering that $i_a + i_b + i_c = 0$ all the time, we can further get,

$$\begin{cases} 3L\dfrac{di_a}{dt} + 3Ri_a + \dfrac{v_{dc}}{2}(S_{ab} - S_{ca}) = v_{ab} - v_{ca} \\ 3L\dfrac{di_b}{dt} + 3Ri_b + \dfrac{v_{dc}}{2}(S_{bc} - S_{ab}) = v_{bc} - v_{ab} \\ 3L\dfrac{di_c}{dt} + 3Ri_c + \dfrac{v_{dc}}{2}(S_{ca} - S_{bc}) = v_{ca} - v_{bc} \end{cases} \tag{5}$$

where v_{ab}, v_{bc}, v_{ca}, S_{ab}, S_{bc}, and S_{ca} are the line voltages and line switching functions, respectively.

Combining (3), (4), and (5), we can further get,

$$\begin{cases} L\dfrac{di_a}{dt} + Ri_a + \dfrac{v_{dc}}{2}(S_a - \Delta S) = v_a - \Delta v \\ L\dfrac{di_b}{dt} + Ri_b + \dfrac{v_{dc}}{2}(S_b - \Delta S) = v_b - \Delta v \\ L\dfrac{di_c}{dt} + Ri_c + \dfrac{v_{dc}}{2}(S_c - \Delta S) = v_c - \Delta v \end{cases} \tag{6}$$

where ΔS and Δv are defined zero sequence switching function and zero sequence voltage, respectively.

Then the potential difference v_{ON} can be descripted as,

$$\begin{cases} v_{ON} = \Delta v - \dfrac{v_{dc}}{2}\Delta S \\ \Delta v = \dfrac{v_a + v_b + v_c}{3} \\ \Delta S = \dfrac{S_a + S_b + S_c}{3} \end{cases} \tag{7}$$

B. DQ COORDINATE MODEL

To make the Vienna rectifier operate stably, the synchronous rotation coordinate is adopted. The currents, line voltages, and line switching functions are transformed as follow,

$$\begin{cases} \begin{pmatrix} i_d \\ i_q \end{pmatrix} = T_1 \begin{pmatrix} i_a \\ i_b \\ i_c \end{pmatrix}, \\ T_1 = \dfrac{2}{3} \\ \quad \begin{pmatrix} \cos(\omega t) & \cos(\omega t - 2\pi/3) & \cos(\omega t + 2\pi/3) \\ -\sin(\omega t) & -\sin(\omega t - 2\pi/3) & -\sin(\omega t + 2\pi/3) \end{pmatrix} \end{cases} \tag{8}$$

$$\begin{cases} \begin{pmatrix} S_d \\ S_q \end{pmatrix} = T_2 \begin{pmatrix} S_{ab} \\ S_{bc} \\ S_{ca} \end{pmatrix}, \begin{pmatrix} v_d \\ v_q \end{pmatrix} = T_2 \begin{pmatrix} v_{ab} \\ v_{bc} \\ v_{ca} \end{pmatrix}, \\ T_2 = \dfrac{2}{3} \\ \quad \begin{pmatrix} \cos(\omega t + \pi/6) & \cos(\omega t - \pi/2) & \cos(\omega t + 5\pi/6) \\ -\sin(\omega t + \pi/6) & -\sin(\omega t - \pi/2) & -\sin(\omega t + 5\pi/6) \end{pmatrix} \end{cases} \tag{9}$$

where i_d, i_q, v_d, v_q, S_d, and S_q are dq coordinate currents, line voltages and line switching functions, respectively. $\boldsymbol{T}_1$ and $\boldsymbol{T}_2$ are the transformation matrices from abc coordinate to dq coordinate. Combining (6), (8), and (9), we can further get,

$$\begin{cases} L\dfrac{di_d}{dt} + Ri_d - \omega L i_q + \dfrac{\sqrt{3}}{6} S_d v_{dc} = \dfrac{v_d}{\sqrt{3}} \\ L\dfrac{di_q}{dt} + \omega L i_d + Ri_q + \dfrac{\sqrt{3}}{6} S_q v_{dc} = \dfrac{v_q}{\sqrt{3}} \\ \dfrac{2C}{3}\dfrac{dv_{dc}}{dt} - \dfrac{\sqrt{3}}{6} S_d i_d - \dfrac{\sqrt{3}}{6} S_q i_q + \dfrac{2}{3R_L} v_{dc} = 0 \end{cases} \tag{10}$$

C. EULER LAGRAN MODEL

We can further get the mathematical model of the Vienna rectifier in EL form,

$$\boldsymbol{M}\dot{\boldsymbol{X}} + \boldsymbol{J}\boldsymbol{X} + \boldsymbol{R}\boldsymbol{X} = \boldsymbol{V} \tag{11}$$

where $\boldsymbol{M}$ is a positive definite symmetric coefficient matrix, i.e. $\boldsymbol{M}^{\mathrm{T}} = \boldsymbol{M}$. $\boldsymbol{J}$ is an anti-symmetric coefficient matrix, i.e. $\boldsymbol{J}^{\mathrm{T}} = -\boldsymbol{J}$. $\boldsymbol{R}$ is a positive coefficient matrix, i.e. $\boldsymbol{R}^{\mathrm{T}} = \boldsymbol{R}$, and it satisfies $\boldsymbol{R} > 0$, which means that the converter has dissipative character. $\boldsymbol{X}$ is the state variable vector, and $\boldsymbol{V}$ is the control input variable vector.

$$\boldsymbol{M} = \begin{pmatrix} L & 0 & 0 \\ 0 & L & 0 \\ 0 & 0 & \dfrac{2C}{3} \end{pmatrix}, \boldsymbol{R} = \begin{pmatrix} R & 0 & 0 \\ 0 & R & 0 \\ 0 & 0 & \dfrac{2}{3R_L} \end{pmatrix},$$
$$\boldsymbol{X} = \begin{pmatrix} i_d \\ i_q \\ v_{dc} \end{pmatrix} \tag{12}$$
$$\boldsymbol{J} = \begin{pmatrix} 0 & -\omega L & \dfrac{\sqrt{3}}{6} S_d \\ \omega L & 0 & \dfrac{\sqrt{3}}{6} S_q \\ -\dfrac{\sqrt{3}}{6} S_d & -\dfrac{\sqrt{3}}{6} S_q & 0 \end{pmatrix}, \boldsymbol{V} = \begin{pmatrix} \dfrac{v_d}{\sqrt{3}} \\ \dfrac{v_q}{\sqrt{3}} \\ 0 \end{pmatrix} \tag{13}$$

It is assumed that the system storage energy function is,

$$\boldsymbol{H}\ \mathcal{D}\ \frac{1}{2}\boldsymbol{X}^{\mathrm{T}}\boldsymbol{M}\boldsymbol{X} = \frac{1}{2}(Li_d^2 + Li_q^2 + \frac{2C}{3}v_{dc}^2) \geq 0 \tag{14}$$

Then we can get the differential of the function $\boldsymbol{H}(\boldsymbol{X})$ as,

$$\begin{aligned} \dot{H} &= i_d L\frac{di_d}{dt} + i_q L\frac{di_q}{dt} + v_{dc}\frac{2C}{3}\frac{dv_{dc}}{dt} \\ &= \boldsymbol{X}^{\mathrm{T}}\boldsymbol{M}\dot{\boldsymbol{X}} = \boldsymbol{X}^{\mathrm{T}}(\boldsymbol{V} - \boldsymbol{J}\boldsymbol{X} - \boldsymbol{R}\boldsymbol{X}) \\ &= \boldsymbol{X}^{\mathrm{T}}\boldsymbol{V} - \boldsymbol{X}^{\mathrm{T}}\boldsymbol{R}\boldsymbol{X} = \boldsymbol{X}^{\mathrm{T}}\boldsymbol{V} - \boldsymbol{Q}(\boldsymbol{X}) \end{aligned} \tag{15}$$

It can be seen that $\boldsymbol{H}(\boldsymbol{X})$ is positive semidefinite and $\boldsymbol{Q}(\boldsymbol{X})$ is positive definite. If the output variables matrix $\boldsymbol{Y}$ is equal to $\boldsymbol{X}$, the energy supply rate $\boldsymbol{X}^{\mathrm{T}}\boldsymbol{V}$ is valid to any input variable. According to the passivity-based control principle, the Vienna rectifier is strictly passive.

IV. PBC WITH ADRC CONTROLLER DESIGN

A. INNER LOOP PBC CURRENT CONTROL

The PBC control object is that $\boldsymbol{X}$ converges to $\boldsymbol{X}^* = (i_d^* i_q^* v_{dc}^*)^{\mathrm{T}}$, and the error vector $\boldsymbol{X}_e = \boldsymbol{X} - \boldsymbol{X}^*$ converges to $\boldsymbol{0}$, where i_d^*, i_q^*, and v_{dc}^* are ac currents and dc voltage objects, respectively. In order to accelerate $\boldsymbol{X}_e$ converges to $\boldsymbol{0}$, the damping injecting matrix $\boldsymbol{R}_d = \mathrm{diag}\{r_{11} r_{11}\ r_{22}\}$ is used, where r_{11} and r_{22} are positive damping coefficients. And the mathematical module with state vector $\boldsymbol{X}$ can be further descripted by the module with error vector $\boldsymbol{X}_e$ as,

$$\boldsymbol{M}\dot{\boldsymbol{X}}_e + (\boldsymbol{R}\ \boldsymbol{C}\ \boldsymbol{R}_d)\boldsymbol{X}_e = \boldsymbol{V} - (\boldsymbol{M}\dot{\boldsymbol{X}}* + \boldsymbol{J}\boldsymbol{X} + \boldsymbol{R}\boldsymbol{X} * - \boldsymbol{R}_d\boldsymbol{X}_e) \tag{16}$$

And the line voltages based PBC control equation can be selected as,

$$\boldsymbol{V} = \boldsymbol{M}\dot{\boldsymbol{X}}* + \boldsymbol{J}\boldsymbol{X} + \boldsymbol{R}\boldsymbol{X} * - \boldsymbol{R}_d\boldsymbol{X}_e \tag{17}$$

According to (10) and (17), we can get the Vienna rectifier PBC control equations as,

$$\begin{cases} S_d = \dfrac{v_d - \sqrt{3}[L\frac{di_d^*}{dt} + Ri_d^* - \omega L i_q - R_{11}(i_d - i_d^*)]}{v_{dc}/2} \\ S_q = \dfrac{v_q - \sqrt{3}[L\frac{di_q^*}{dt} + Ri_q^* + \omega L i_d - R_{11}(i_q - i_q^*)]}{v_{dc}/2} \end{cases} \tag{18}$$

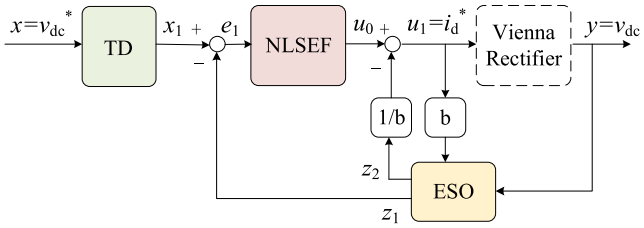

FIGURE 2. The first order ADRC of dc voltage control.

And then we can further get the line and phase switching function as,

$$\begin{cases} \begin{pmatrix} S_{ab} \\ S_{bc} \\ S_{ca} \end{pmatrix} = \boldsymbol{T}_2^{-1} \begin{pmatrix} S_d \\ S_q \end{pmatrix}, \\ \begin{pmatrix} S_a \\ S_b \\ S_c \end{pmatrix} = \frac{1}{3} \begin{pmatrix} 1 & 0 & -1 \\ -1 & 1 & 0 \\ 0 & -1 & 1 \end{pmatrix} \begin{pmatrix} S_{ab} \\ S_{bc} \\ S_{ca} \end{pmatrix} \\ \quad + \begin{pmatrix} \Delta S \\ \Delta S \\ \Delta S \end{pmatrix}, \Delta S = \dfrac{2\Delta v}{v_{dc}} \end{cases} \tag{19}$$

B. OUTER LOOP ADRC VOLTAGE CONTROL

To implement PBC, the dq coordinate reference current i_d^* and i_q^* are used. In general, i_q^* is equal to 0 to realize unity power factor or be set according to reactive power compensation requirement, and i_d^* is get from the outer voltage loop, and a traditional PI controller is normally used. To improve the static and dynamic performance, an ADRC controller can be also used to compensate disturbance for the system. The ADRC can be divided into three parts as tracking differentiator (TD), extended state observer (ESO) and nonlinear state errors feedback (NLSEF) [33], [34]. Thus, the controller design can be divided into TD, ESO and NLSEF design, respectively, as depicted in the Fig.2.

1) DESIGN OF TD

A TD module can improve the respond speed and voltage overshoot effectively, and a first-order TD module can be selected to implement the dc voltage reference as,

$$\dot{x}_1 = -\alpha_1 \sin \mathrm{sgn}(x_1 - v_{dc}^*, \delta_1) \tag{20}$$

where x_1 is the tracking signal of the dc voltage reference. α_1 is the TD speed coefficient, and the greater α_1, the higher tracking speed. δ_1 is the TD non-linear function coefficient, and the TD non-linear function can be descripted as,

$$\sin \mathrm{sgn}(A, \delta_1) = \begin{cases} 1, & A > \delta_1 \\ \sin \dfrac{\pi A}{2\delta_1}, & |A| < \delta_1 \\ -1, & A < -\delta_1 \end{cases} \tag{21}$$

2) DESIGN OF ESO

An ESO module can realize the real-time dc voltage estimation, and the inputs of ESO are input and output of Vienna rectifier, i.e. the d axial current reference i_d^* and dc voltage v_{dc}, the outputs of ESO are estimated state and expanded state. The implementation process of ESO is shown as,

$$\begin{cases} e = z_1 - v_{dc} \\ \dot{z}_1 = z_2 - \beta_1 fal(e, \alpha_2, \delta_2) + b i_d^* \\ \dot{z}_2 = -\beta_2 fal(e, \alpha_3, \delta_3) \end{cases} \tag{22}$$

where z_1 and z_2 are the real-time estimation value and the expanded state value, respectively. e is the error between output estimation and input signal. b is a feedback coefficient of the ADRC output. β_1 and β_2 are weight coefficients, and $fal()$ is a non-linear smooth function, and its definition is,

$$fal(e, \alpha, \delta) = \begin{cases} e^{\alpha}, & e > \delta \\ \dfrac{e}{\delta^{1-\alpha}}, & |e| < \delta \\ -(-e)^{\alpha}, & e < -\delta \end{cases} \tag{23}$$

where α is a tracking coefficient, which ranges from 0 to 1, and the smaller the tracking coefficient, the faster the tracking speed. δ is a filter effect coefficient, and the greater filter effect coefficient, the better the filter effect, but the tracking delay time will be increased, so a suitable filter effect coefficient should be selected in the application.

3) DESIGN OF NLSEF

The output of NLSEF is determined by the difference between the reference estimated value and the actual estimated value, i.e.,

$$\begin{cases} e_1 = x_1 - z_1 \\ i_d^* = \beta_3 fal(e_1, \alpha_4, \delta_4) - \dfrac{z_2}{b} \end{cases} \tag{24}$$

where α_4 and δ_4 are tracking coefficient and filter effect coefficient, respectively, and β_3 is a weight coefficient.

C. DC BALANCE IMPLEMENTATION

In the previous analysis, it is assumed that the voltages of the upper and lower capacitors are completely balanced, but in fact some dc voltage balance control must be adopted to balance the voltages of the upper and lower capacitors. The zero-sequence voltage injection scheme is used in the study, and the injected voltage can be selected as,

$$v_{zsvi} = signn(-i_i \Delta v_{dc} C) \Delta v_{dc} C, \quad i = a, b, c \tag{25}$$

where v_{zsvi} is the zero-sequence voltage, sgnn(x) is a sign function, when $x \geq 0$, sgnn(x) is equal to 1, and when $x < 0$, sgnn(x) is equal to 0. It can be seen that only when the current direction isn't consistent with dc voltage difference's polarity, the zero-sequence voltage is injected, and the magnitude of the zero-sequence voltage is decided by dc voltage difference and capacitance value. Then the Vienna rectifier ac voltages

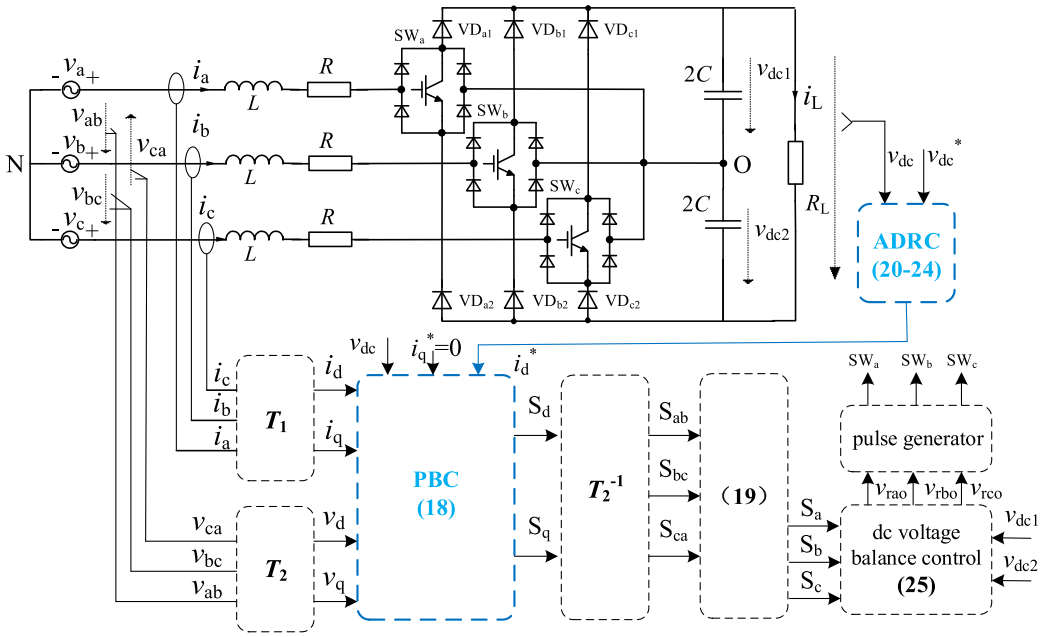

FIGURE 3. The PBC with ADRC control diagram of the Vienna rectifier.

TABLE 1. Main circuit parameters of Vienna rectifier.

Parameters	Value
rated ac voltage (V)	380
rated output voltage (V)	800
ac inductance L (mH)	1.3
dc-link capacitor (μF)	550
Switching frequency (kHz)	10.0
load inductance (mH)	1.0
load resistance (Ω)	64

TABLE 2. Control coefficients of Vienna rectifier.

Coefficients	Value
PI control k_p	0.0005
PI control k_i	10.7
ADRC control TD α_1	10000
ADRC control TD δ_1	0.01
ADRC control ESO b	1.5
ADRC control ESO β_1	200
ADRC control ESO β_2	60
ADRC control NLSEF β_3	60

can be got, and modulated according to space vector modulation or sinusoidal pulse width modulation to drive the power switches SW_a, SW_b, and SW_c.

$$v_{rio} = \frac{S_i v_{dc}}{2} + v_{zsvi}, \quad i = a, b, c \tag{26}$$

The ADRC control is used in outer voltage loop to generate active reference current i_d^*, and the line voltage based PBC control is used in inner current loop to get output voltage reference v_{rio}. The PBC with ADRC control diagram of the Vienna rectifier is illustrated in the Fig. 3.

V. SIMULATION VERIFICATION

To verify the proposed PBC with ADRC control strategy, simulations under balanced and different unbalanced grid conditions are carried out in SIMULINK. The main circuit parameters of the Vienna rectifier are shown in Table 1, and the control coefficients are listed in the Table 2.

A. BANLANCED GRID SIMULATION

In the Fig.4, the three-phase grid has balanced voltages with perfect sinusoidal waves, same amplitude and same phase difference. The Vienna rectifier currents are also balanced

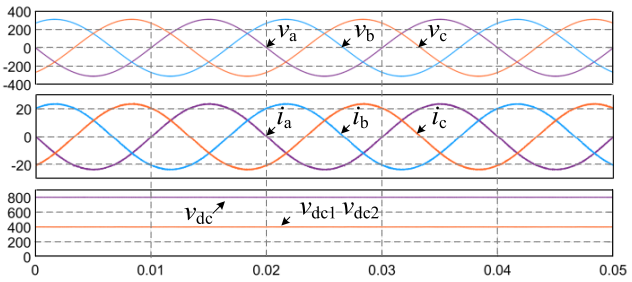

FIGURE 4. Waveforms under balanced grid condition.

with perfect sinusoidal waves, same amplitude and same phase difference, and the currents are in phase with their corresponding voltages. The dc voltage is always stable at 800V, and the upper and lower capacitors share the same voltage. It proves that the proposed PBC with ADRC control strategy can operate the Vienna rectifier stably with unity power factor and low total harmonic distortion (THD) under balanced grid condition.

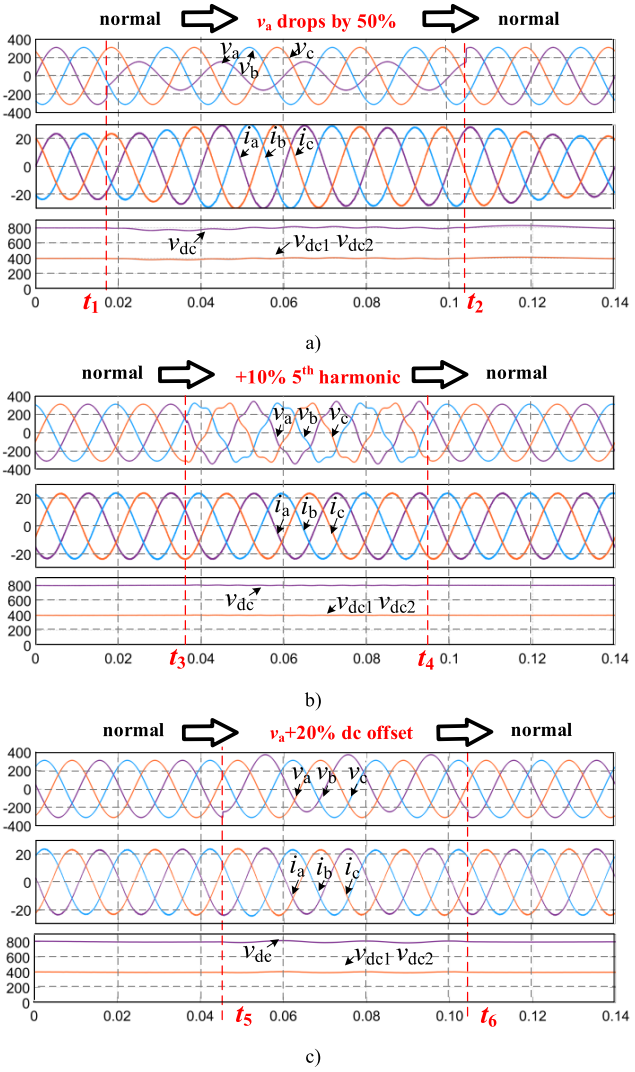

FIGURE 5. Waveforms under unbalanced grid condition. a) Voltage sag of phase A. b) With fifth harmonic voltage of phase A, B, and C simultaneously. c) With dc offset of phase A.

B. UNBALANCED GRID SIMULATION

In the Fig.5, voltages and currents waveforms under different unbalanced grid conditions are shown. In the Fig. 5a, the three-phase grid has balanced voltages at first. At the time t_1, there is a voltage drop of phase A from 220V to 110V, the Vienna rectifier currents are still balanced perfect sinusoidal waves, the currents amplitudes increase gradually, and the currents are still in phase with corresponding voltages. At the time t_2, the voltage of phase A returns to the normal value, and the Vienna rectifier currents restore to the original values gradually. In the transient process, there are some dc voltage fluctuations, and the transient time is less than 0.02s.

In the Fig. 5b,, the three-phase grid has balanced voltages at first. At the time t_3, the fifth harmonic voltages, whose amplitudes are 10% of the fundamental voltage amplitudes, are injected to the voltages of phase A, B, and C respectively.

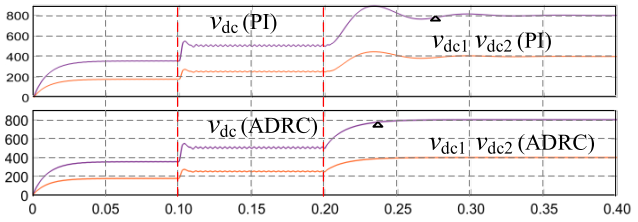

FIGURE 6. Waveforms of dc voltages in PI and ADRC control respectively.

Then, the Vienna rectifier currents are consistently balanced perfect sinusoidal waves without harmonics, phase shift and amplitude change. At the time t_4, the fifth harmonic voltages are reset to 0, and the Vienna rectifier currents have no obvious change. In the transient process, the dc voltages have no any obvious changes, and it means that the grid harmonics have no influence to the Vienna rectifier.

In the Fig. 5c, the grid voltages are balanced at first. At the time t_5, the positive dc offset, whose amplitude is 20% of the fundamental voltage amplitudes, is injected to voltage of phase A. Then, the Vienna rectifier currents are consistently balanced perfect sinusoidal waves without dc offset, phase shift and amplitude change. At the time t_6, the dc offset is reset to 0, and the Vienna rectifier currents have no obvious change. In the transient process, the dc voltages have only very small fluctuations.

From the simulation results, we conclude that in whether voltage drop, harmonic injection or dc offset unbalanced grid conditions, the proposed PBC with ADRC control strategy can operate Vienna rectifier stably with high power quality and good output performance, the grid currents are always balanced perfect sinusoidal waves with unity power factor and low THD, and the output voltage is always stable at the set value.

C. ADRC SIMULATION

DC voltages waveforms in PI and ADRC control are shown respectively in Fig. 6. At the time $t = 0$, the main circuit breaker is switched on, the power supply is starting to charge the dc capacitor, the dc voltages increase gradually, and the output voltage reaches 360V ultimately. At the time $t = 0.1$s, the soft start resistor is bypassed, the dc voltages increase rapidly, and the output voltage reaches 515V finally. At the time $t = 0.2$s, the controller is starting to operate, and the output voltage begins to increase and be stabilized at 800V after a period of transient time. It can be seen that the PI control has about 0.07s response time with voltage overshoot of 100V, but the ADRC control has only 0.03s response time without voltage overshoot. And it shows that the ADRC control has better performance compared with the PI control.

VI. EXPERIMENTAL VERIFICATION

In order to further verify the effectiveness of the proposed PBC with ADRC control strategy, a downsize 5 kW Vienna

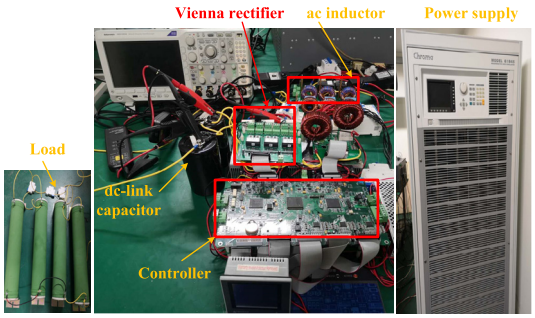

FIGURE 7. The Vienna rectifier prototype.

TABLE 3. Prototype main circuit parameters.

Parameters	Value
Rated power (kW)	5.0
Rated ac voltage (V)	150
Rated output voltage (V)	300
AC inductance L (mH)	1.0
DC-link capacitor (μF)	2350
Switching frequency (kHz)	12.8
Switches of Vienna rectifier	10-FZ071SA050SM02

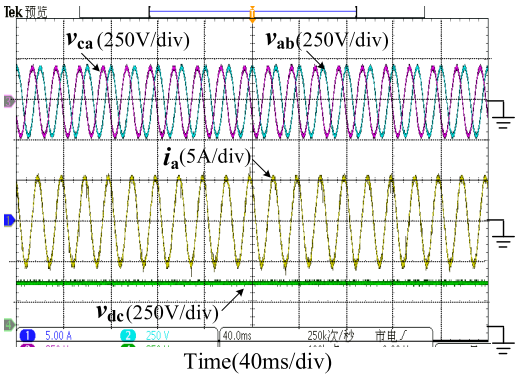

FIGURE 8. Waveforms under balanced grid condition.

rectifier prototype is built, as shown in Fig. 7. The main circuit parameters are shown in Table 3, experiments of balanced grid condition and various unbalanced grid condition are also carried out in the prototype.

Fig. 8 gives voltages and current waveforms of the Vienna rectifier under balanced grid condition. The proposed PBC with ADRC strategy can operate the Vienna rectifier stably with perfect sinusoidal current and unity power factor, and stabilize output voltage to drive the load at the same time.

In the Fig. 9a, at the first, the Vienna rectifier operates stably under balanced grid condition. At the time t_1, there is a voltage drop of phase B from 87V to 40V, i.e. the line voltages v_{ab} and v_{bc} change from 150V to 120V, and the line voltage v_{ca} has no change. It can be seen that the phase current i_b increases gradually with perfect sinusoidal wave and no

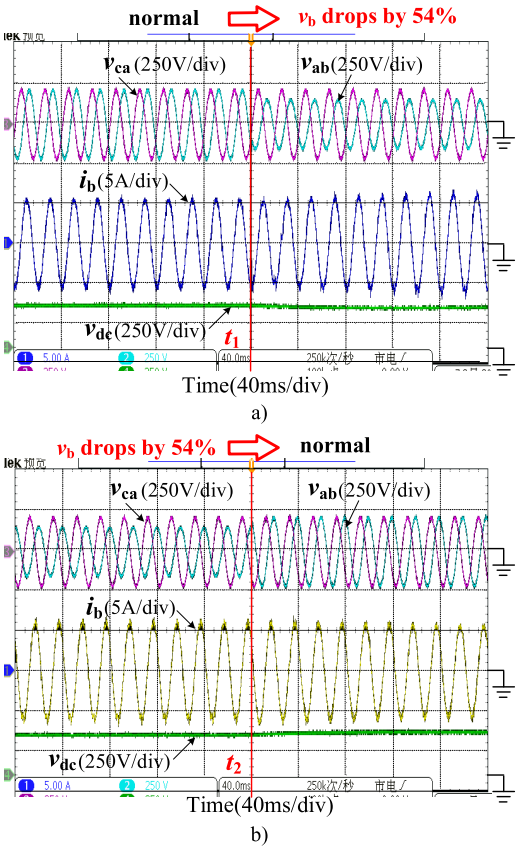

FIGURE 9. Waveforms under unbalanced grid condition with voltage drop. a) To unbalanced grid condition with phase B voltage drop. b) From unbalanced grid condition with phase B voltage drop.

phase angle shift. In the Fig. 9b, at the time t_2, the voltages restore to balanced grid condition, and the phase current i_b decreases gradually with perfect sinusoidal wave and no phase angle shift. In all these transient processes, the output voltage remains constant to drive the load all the time, and the grid currents are consistently perfect sinusoidal waves with unity power factor.

In the Fig. 10a, at the first, the Vienna rectifier operates stably under balanced grid condition. At the time t_3, the fifth harmonic voltage, whose amplitude is 20% of the fundamental voltage amplitude, is superposed to voltage of phase B, the THD of line voltages v_{ab} and v_{bc} increase, and the THD of line voltage v_{ca} has no change. It can be seen that the phase currents i_a and i_b increase gradually with no fifth harmonic, no phase angle shift and no obvious current THD increase, and the Vienna rectifier currents are also balanced all the time. In the Fig. 10b, at the time t_4, the fifth harmonic voltage is reset to 0, and the grid voltages have 90°-lead angle shifts at the same time. It can be seen that the phase currents i_a and i_b have also 90°-lead angle shifts, the Vienna rectifier currents enter steady state after about 38ms transient process, and the currents begin to increase gradually. In the transient process, the Vienna rectifier currents are always controlled within the rated current range without overcurrent.

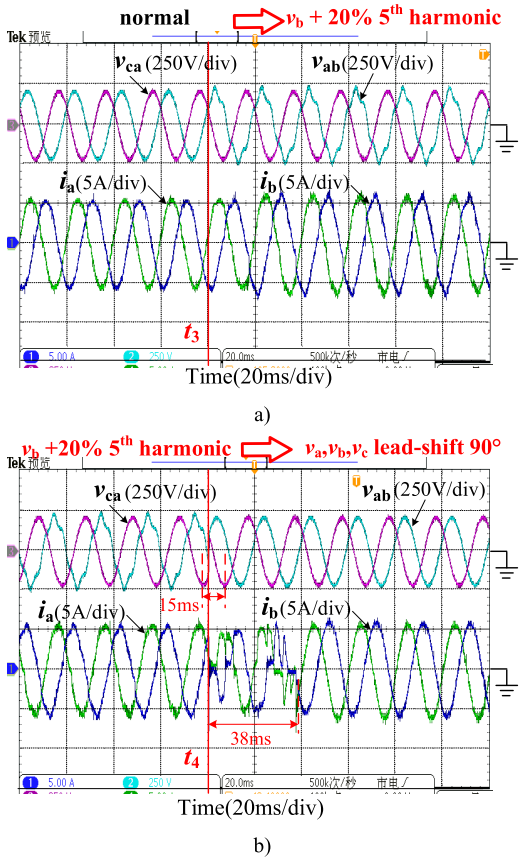

FIGURE 10. Waveforms under unbalanced grid condition with harmonic voltage superpose of phase B. a) To unbalanced grid condition with harmonic voltage. b) From unbalanced grid condition with harmonic voltage.

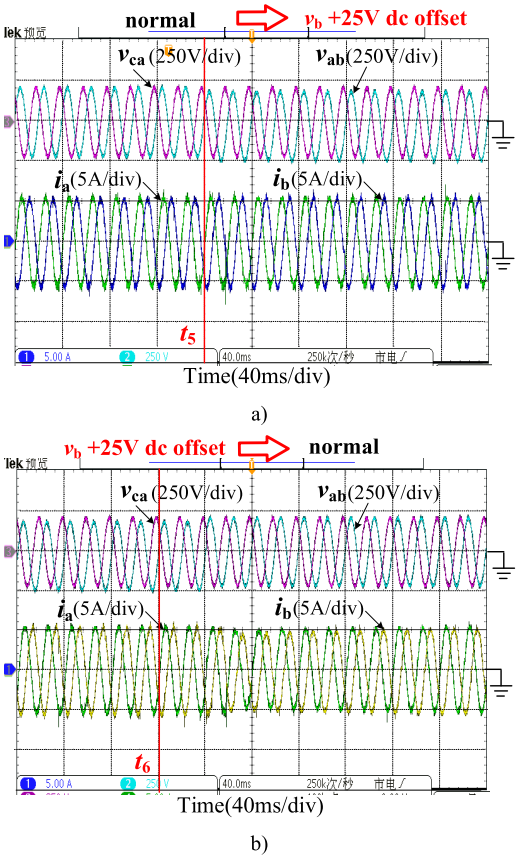

FIGURE 11. Waveforms under unbalanced grid condition with dc offset of phase B. a) To unbalanced grid condition with dc offset. b) From unbalanced grid condition with dc offset.

And it validates that the proposed solution has not only good steady state performance, but also good transient process performance.

In the Fig. 11a, the Vienna rectifier operates stably under balanced grid condition at first. At the time t_5, the dc offset of 25V is superposed to phase B voltage, the line voltage v_{ab} has a negative shift, and the line voltage v_{ca} has no change. It can be seen that the Vienna rectifier currents i_a and i_b are balanced all the time without obvious amplitude change and phase angle shift. In the Fig. 11b, at the time t_6, the dc offset is reset to 0, and the Vienna rectifier currents are also balanced all the time without obvious amplitude change and phase angle shift.

From the experimental results, we conclude that the proposed solution can ensure the Vienna rectifier's stable operation with good output performance and high power quality under whatever balanced grid condition or various unbalanced grid conditions, which includes voltage drop, harmonic distortion and dc offset injection. The experimental results give strong support to the analysis above given and strengthen the simulation results.

VII. CONCLUSION

This study proposes a practical control strategy based on PBC with ADRC for the Vienna rectifier. The proposed control strategy adopts line voltage based PBC in inner current loop and ADRC in outer voltage loop, there is no need of negative sequence transformation, harmonic and dc elements detection under unbalanced conditions, there is only need of instantaneous voltages and currents detections and controls, and the control strategy has the advantage of easy implementation, less consuming time, good performance, strong robustness and fast track performance.

REFERENCES

[1] J. W. Kolar and F. C. Zach, "A novel three-phase utility interface minimizing line current harmonics of high-power telecommunications rectifier modules," *IEEE Trans. Ind. Electron.*, vol. 44, no. 4, pp. 456–467, Aug. 1997.

[2] J. W. Kolar, U. Drofenik, and F. C. Zach, "VIENNA rectifier II—A novel single-stage high-frequency isolated three-phase PWM rectifier system," *IEEE Trans. Ind. Electron.*, vol. 46, no. 4, pp. 674–691, Aug. 1999.

[3] A. von Jouanne and B. Banerjee, "Assessment of voltage unbalance," *IEEE Trans. Power Del.*, vol. 16, no. 4, pp. 782–790, Oct. 2001.

[4] X. Cai, L. Li, C. Zhao, and T. Li, "Passivity-based control of HVDC transmission system based on modular multilevel converter under unbalanced grid conditions," in *Proc. 2nd IET Renew. Power Gener. Conf. (RPG)*, Beijing, China, Sep. 2013, pp. 1–4.

[5] M. Guan and Z. Xu, "Modeling and control of a modular multilevel converter-based HVDC system under unbalanced grid conditions," *IEEE Trans. Power Electron.*, vol. 27, no. 12, pp. 4858–4867, Dec. 2012.
[6] P. Rodriguez, A. Luna, M. Ciobotaru, R. Teodorescu, and F. Blaabjerg, "Advanced grid synchronization system for power converters under unbalanced and distorted operating conditions," in *Proc. 32nd Annu. Conf. IEEE Ind. Electron. (IECON)*, Nov. 2006, pp. 5173–5178.
[7] C. Bing, M. Hui, X. Yunxiang, and W. Yingpin, "Sliding mode and predictive current control for vienna-type rectifiers," in *Proc. 18th Int. Conf. Electr. Mach. Syst. (ICEMS)*, Oct. 2015, pp. 340–344.
[8] S. Gadelovitz and A. Kuperman, "Modeling and classical control of unidirectional vienna rectifiers," in *Proc. Electr. Power Qual. Supply Rel.*, Jun. 2012, pp. 1–4.
[9] E.-J. Qi, Z. Luo, H. Chen, and G.-R. Zhu, "Modelling and control of single phase VIENNA rectifier," in *Proc. Int. Conf. Ind. Informat. Comput. Technol., Intell. Technol., Ind. Inf. Integr. (ICIICII)*, Dec. 2016, pp. 286–289.
[10] M. E. Meral and D. Çelík, "A comprehensive survey on control strategies of distributed generation power systems under normal and abnormal conditions," *Annu. Rev. Control*, vol. 47, pp. 112–132, 2019.
[11] D. Çelík and M. E. Meral, "A flexible control strategy with overcurrent limitation in distributed generation systems," *Int. J. Electr. Power Energy Syst.*, vol. 104, pp. 456–471, Jan. 2019.
[12] X. Du and R. Wang, "Control strategy of negative sequence current for the grid-connection converter under the unbalanced grid condition," in *Proc. 34th Chin. Control Conf. (CCC)*, Jul. 2015, pp. 9066–9071.
[13] K. Li, J. Liu, Z. Wang, and B. Wei, "Strategies and operating point optimization of STATCOM control for voltage unbalance mitigation in three-phase three-wire systems," *IEEE Trans. Power Del.*, vol. 22, no. 1, pp. 413–422, Jan. 2007.
[14] X. Zhu and Y. Zhang, "Control strategy of DC microgrid under unbalanced grid voltage," in *Proc. IEEE 8th Int. Power Electron. Motion Control Conf. (IPEMC-ECCE Asia)*, May 2016, pp. 1725–1731.
[15] Y. Teng, C. Xiong, C. Li, Q. Hui, and Y. Zhu, "Grid-connected PV power plant LCL filter based on PI and PR control strategy," in *Proc. IEEE Adv. Inf. Technol., Electron. Autom. Control Conf. (IAEAC)*, Dec. 2015, pp. 1191–1196.
[16] Y. Liu, R. Bai, D. Wang, W. Ma, and L. Wang, "Proportional-resonant control method of three-phase grid-connected inverter," in *Proc. 26th Chin. Control Decis. Conf. (CCDC)*, May 2014, pp. 4797–4800.
[17] H. Sun, Y. Sun, L. Zhang, J. Cai, and D. Zhang, "Three single-phase control of NPC three-level photovoltaic grid-connected inverter based on quasi-PR control," in *Proc. Int. Conf. Electr. Mach. Syst. (ICEMS)*, Oct. 2013, pp. 1603–1608.
[18] H. C. Nannam and A. Banerjee, "A detailed modeling and comparative analysis of hysteresis current controlled vienna rectifier and space vector pulse width modulated vienna rectifier in mitigating the harmonic distortion on the input mains," in *Proc. IEEE Int. Conf. Ind. Eng. Eng. Manage. (IEEM)*, Bangkok, Thailand, Dec. 2018, pp. 371–375.
[19] J. Wang, H. Li, and L. Wang, "Direct power control system of three phase boost type PWM rectifiers," in *Proc. CSEE*, 2006, vol. 26, no. 18, pp. 54–60.
[20] J.-S. Lee and K.-B. Lee, "Predictive control of vienna rectifiers for PMSG systems," *IEEE Trans. Ind. Electron.*, vol. 64, no. 4, pp. 2580–2591, Apr. 2017.
[21] Y.-D. Kwon, J.-H. Park, K. M. Kim, and K.-B. Lee, "Line current improvement of three-phase four-wire vienna rectifier using dead-beat control," in *Proc. IEEE Conf. Energy Convers. (CENCON)*, Oct. 2017, pp. 49–54.
[22] R. Ortega and M. W. Spong, "Adaptive motion control of rigid robots: A tutorial," in *Proc. 27th IEEE Conf. Decis. Control*, Dec. 1988, pp. 1575–1584.
[23] J. Li, X. Lv, B. Zhao, Y. Zhang, Q. Zhang, and J. Wang, "Research on passivity based control strategy of power conversion system used in the energy storage system," *IET Power Electron.*, vol. 12, no. 3, pp. 392–399, Mar. 2019.
[24] J. Li, M. Wang, Y. Zhao, J. Wang, D. Yang, and X. Lv, "Passivity-based control of the hybrid rectifier for medium and high-power application," *IET Power Electron.*, vol. 12, no. 15, pp. 4070–4078, Dec. 2019.
[25] J. Wang, X. Mu, and Q.-K. Li, "Study of passivity-based decoupling control of T-NPC PV grid-connected inverter," *IEEE Trans. Ind. Electron.*, vol. 64, no. 9, pp. 7542–7551, Sep. 2017.
[26] X. Mu, J. Wang, W. Wu, and F. Blaabjerg, "A modified multifrequency passivity-based control for shunt active power filter with model-parameter-adaptive capability," *IEEE Trans. Ind. Electron.*, vol. 65, no. 1, pp. 760–769, Jan. 2018.
[27] J. Wang and X. Mu, "Hybrid passivity based control of voltage source PWM rectifiers under unbalanced voltage conditions," *Trans. China Electrotech. Soc.*, vol. 30, no. 8, pp. 159–166, Apr. 2015.
[28] J. Han, *Active Disturbance Rejection Control Technique—The Technique for Estimating and Compensating the Uncertainties*. Beijing, China: China National Defense Industry Press, 2016.
[29] B. Sun and Z. Gao, "A DSP-based active disturbance rejection control design for a 1-kW H-bridge DC–DC power converter," *IEEE Trans. Ind. Electron.*, vol. 52, no. 5, pp. 1271–1277, Oct. 2005.
[30] Q. Zheng, L. Dong, D. Hui Lee, and Z. Gao, "Active disturbance rejection control for MEMS gyroscopes," *IEEE Trans. Control Syst. Technol.*, vol. 17, no. 6, pp. 1432–1438, Nov. 2009.
[31] H. Sira-Ramirez, J. Linares-Flores, C. Garcia-Rodriguez, and M. A. Contreras-Ordaz, "On the control of the permanent magnet synchronous motor: An active disturbance rejection control approach," *IEEE Trans. Control Syst. Technol.*, vol. 22, no. 5, pp. 2056–2063, Sep. 2014.
[32] X. Chang, Y. Li, W. Zhang, N. Wang, and W. Xue, "Active disturbance rejection control for a flywheel energy storage system," *IEEE Trans. Ind. Electron.*, vol. 62, no. 2, pp. 991–1001, Feb. 2015.
[33] H. Zhu and J. Wang, "Research on passivity based control and active disturbance rejection control for MMC-UPQC," in *Proc. 43rd Annu. Conf. IEEE Ind. Electron. Soc. (IECON)*, Oct. 2017, pp. 6425–6430.
[34] S. Li and H. Xiong, "Active disturbance rejection control of single phase grid connected inverter," in *Proc. IEEE Int. Conf. Mechatronics Autom.*, Aug. 2016, pp. 2344–2348.

JIANGUO LI (Member, IEEE) was born in Hebei, China, in 1975. He received the B.S. degree from the Department of Electrical Engineering (DEE), North China Electric Power University (NCEPU), Baoding, China, in 1997, the M.S. degree from the DEE, Tsinghua University, Beijing, China, in 2005, and the Ph.D. degree from the DEE, NCEPU, Beijing, in 2017. He is currently an Associate Professor with the College of Automation, Beijing Information Science and Technology University. His current research interests include bidirectional dc-dc converter, high-frequency-link power conversion systems, and flexible ac and dc transmission or distribution systems.

MIAN WANG (Student Member, IEEE) was born in Jilin, China, in 1985. He received the M.S. degree in control engineering from the School of Electric power, Inner Mongolia University of Technology, Hohhot, China, in 2017. He is currently pursuing the Ph.D. degree in electrical engineering with Beijing Jiaotong University, Beijing, China. His research interests include power electronics, control, and their applications in dc microgrids.

JING WANG was born in Henan, China, in 1986. She received the M.S. degree from the Department of Electrical Engineering, Huazhong University of Science and Technology, Wuhan, China, in 2012. She is currently working with Shenzhen Power Supply Bureau Co., Ltd. Her current research interests include power system analysis and dc technology.

YAJING ZHANG was born in Hebei, China, in 1984. She received the B.S. and Ph.D. degrees in electrical engineering from Beijing Jiaotong University, China, in 2008 and 2015, respectively. From February 2015 to August 2017, she was a Postdoctoral Researcher of control science and engineering with the Beijing University of Chemical Technology, China. Since 2017, she has been a Lecturer with the College of Automation, Beijing Information and Science Technology University, Beijing, China. Her current research interests include high-efficiency dc-dc converters, high-power density dc-dc converters, and renewable energy applications.

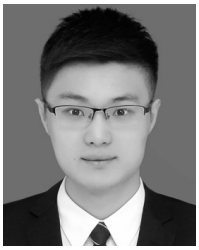

DAOKUAN YANG was born in Jiangsu, China. He received the B.E. degree in automation from the School of Automation, Huaiyin Institute of Technology, Jiangsu, in 2017. He is currently pursuing the master's degree with the Beijing Information Science and Technology University, Beijing, China. His research interests include power electronics and power drives, and nonlinear control of power electronic converter.

JIUHE WANG was born in Jilin, China. He received the B.E. degree in electrical engineering from the School of Electrical and Control Engineering, Liaoning Technical University, Fuxin, China, in 1982, and the Ph.D. degree in control science and engineering from the School of Information Engineering, University of Science and Technology Beijing, Beijing, China, in 2005. He has been a Professor with the School of Automation, Beijing Information Science and Technology University, Beijing. His research interests include nonlinear control of power electronic converter, power quality control, and microgrid.

YUMING ZHAO was born in Jilin, China, in 1978. He received the B.S. and Ph.D. degrees from the Department of Electrical Engineering, Tsinghua University, Beijing, China, in 2001 and 2006, respectively. He is currently a Senior Engineer (professor level) with Shenzhen Power Supply Company, Shenzhen, China. His main research interest includes dc distribution power grid.